Polymer Chemistry

ROYAL SOCIETY OF CHEMISTRY

PAPER

View Article Online
View Journal | View Issue



Cite this: *Polym. Chem.*, 2021, **12**, 4803

# Synthesis and properties of colorless copolyimides derived from 4,4′-diaminodiphenyl ether-based diamines with different substituents†

Ruhe Lian,‡[a,b] Xingfeng Lei, *‡[a,b] Yuyang Xiao,[a] Shuyu Xue,[a,b] Guo Xiong,[a] Zixiang Zhang,[a] Dong Yan[a] and Qiuyu Zhang *[a,b]

Received 10th May 2021,
Accepted 1st August 2021

DOI: 10.1039/d1py00633a

rsc.li/polymers

Colorless polyimide (PI) films with outstanding mechanical and thermal properties are highly demanded in flexible electronics. Herein three 4,4′-diaminodiphenyl ether (**ODA**)-based diamines with different substituents ($-CH_3$, $-CF_3$) and substitution positions (*ortho* and *meta* positions) were synthesized. After reacting with a combination of 1,2,4,5-cyclohexanetetracarboxylic dianhydride (**CHDA**) and 4,4′-(hexafluoroisopropylidene)diphthalic anhydride (**6FDA**) in a typical sequential reaction manner, four highly transparent copolyimide films with excellent mechanical strength, high heat-resistance and superior fracture toughness were fabricated. A copolyimide film made using ***m*-3F-ODA** exhibits a fairly high transmittance at 400 nm of up to 86.8%, tensile strength as high as 102 MPa, tensile modulus of 2.76 GPa and glass transition temperature above 308 °C. The desirable solubility enables the prepared PIs to be readily cast from solution into robust films. All these encouraging results make these PI films potential substrates in place of ultrathin glass in flexible displays.

## Introduction

With the rapid development of flexible electronics, heat-resistant optical flexible polymer thin films in place of ultrathin glass substrates are highly desired.[1–4] As an important class of high-performance engineering plastics, polyimides (PIs) are extensively used in microelectronics and aerospace industries, because of their excellent thermal stability, good chemical resistance and desirable suitability for advanced manufacturing.[5–11] PI thin films are appropriate candidates in place of ultrathin glass substrates for flexible displays. However, aromatic PIs usually suffer from pale yellow to dark brown colorations and poor optical transparency in the visible region, which is an intractable impediment for optical applications.[12,13] Therefore, developing PIs with high optical transparency is of great significance for flexible electronics.

The coloration of PI is generated by the formation of inter- and intramolecular charge transfer complexes (CTCs) and electronic conjugation.[14] In recent years, many efforts have been made to improve the optical transparency of PI films. The introduction of bulky substituents, rigid and noncoplanar segments, asymmetric monomers, or fluorine atoms, and the employment of alicyclic diamines or dianhydrides are successful approaches to obtaining colourless PI films.[15–20] Using alicyclic dianhydrides is the most effective of these methodologies for obtaining colourless PI films.[21–23] Unfortunately, in comparison to aromatic dianhydrides, alicyclic ones show lower reactivity upon reacting with aromatic diamines. Hence, it is relatively difficult to obtain wholly alicyclic dianhydride-based PIs with high molecular weights *via* a conventional two-step method.[24] Although one-step preparation of PIs in phenol solvents is established to enhance the molecular weight of alicyclic dianhydride-based PIs,[22,25] this method is limited by the poor solubility of PIs and, the reaction temperature during the one-pot PI synthesis is fairly high (*e.g.*, 180 °C or higher), inevitably leading to amide or amine oxidation and consequently optical transparency deterioration.[26,27] In addition, compared with wholly aromatic PIs, alicyclic structure insertion will deteriorate the thermal stability. Most recently, Fang and his co-workers reported a novel colourless and transparent poly(ether imide) by using bio-based anethole as starting materials.[28] They firstly synthesized imide-containing diphenols *via* the Diels–Alder reaction and then the diphenols were nucleophilic substituted by decafluorobiphenyl to afford col-

[a]*School of Chemistry and Chemical Engineering, Key Laboratory of Special Functional and Smart Polymer Materials of Ministry of Industry and Information Technology, Northwestern Polytechnical University, Xi'an, Shaanxi, 710072, P. R. China. E-mail: leifeng@nwpu.edu.cn, qyzhang@nwpu.edu.cn; Fax: +86-02988431653; Tel: +86-02988431653*

[b]*School of Chemistry and Chemical Engineering, Key Laboratory of Material Physics and Chemistry under Extraordinary Conditions of Ministry of Education, Northwestern Polytechnical University, Xi'an, Shaanxi, 710072, P. R. China*

†Electronic supplementary information (ESI) available: Characterization including FT-IR, NMR and XRD results. See DOI: 10.1039/d1py00633a

‡These authors contributed equally to this work and should be considered as co-first authors.

ourless poly(ether imide). In Fang's method, the alicyclic moieties were incorporated through a nucleophilic substitution reaction, tactfully avoiding the low reactivity of alicyclic dianhydrides, which opens up a new pathway for fabricating colourless polyimides. It is noteworthy that although the obtained poly(ether imide) exhibited high transparency ($T_{450}$ >85%) and a low CTE (<30 ppm °C$^{-1}$) as well as a high $T_g$ (>360 °C), yet the tensile strength of the thin film (53.3 MPa) as well as its elongation at break (5.4%) should be further improved.[28]

As is known to all, copolymerization of two different dianhydrides is an effective strategy to inhibit CTC formation and would achieve a combination of the desired properties, *i.e.*, increased solubility.[23] However, if two dianhydrides have quite different reactivities, for example, alicyclic dianhydride and aromatic dianhydride, a short block of homopolymer derived from highly active aromatic dianhydride may form first. Hence, it would be difficult to obtain a high molecular weight copolyimide by direct random copolymerization of two distinct dianhydrides with one diamine. It occurs to us whether we can shorten the homopolymer blocks by controlling the dianhydride addition manner. That is, if the alicyclic dianhydride is allowed to firstly react with diamine, further chain growth would be prevented due to its lower reactivity, and a homopolymer block may not be formed. Consequently, amino-terminated macromolecules, rather than oligomers, are prone to formation. After aromatic dianhydride addition, the amino-terminated macromolecules would polymerize with aromatic dianhydride to afford a high molecular weight copolyimide.

In this work, to verify the effectiveness of the sequential addition fashion, an alicyclic dianhydride, 1,2,4,5-cyclohexanetetracarboxylic dianhydride (**CHDA**), was employed by first reacting with four 4,4′-diaminodiphenyl ether (**ODA**)-based diamines in a molar ratio of 1 : 2 and then slowly introducing another aromatic dianhydride, 4,4′-(hexafluoroisopropylidene) diphthalic anhydride (**6FDA**), to prepare several kinds of semi-aromatic copolyimides. The resulting copolyimides are expected to exhibit slight coloration and high optical transparency. Obviously, this elaborate sequential copolymerization would produce copolyimides without homopolymer blocks and the cyclic moiety accounts for 50% of dianhydrides. Thus, desirable heat resistance as well as high mechanical strength can be anticipated. Three **ODA**-based diamines with different substituents (–$CH_3$, –$CF_3$) and substitution positions (*ortho* position and *meta* position) in an aniline ring were prepared to tailor the solubility and optical, mechanical and thermal properties of the resulting copolyimides. Our approach provides a facile modular synthesis concept aiming at high transparency combined with desirable comprehensive performances.

# Experimental section

## Materials

4-Aminophenol (TCI), 5-fluoro-2-nitrotoluene (TCI), 2-bromo-5-nitrotoluene (TCI), 2-chloro-5-nitrobenzotrifluoride (TCI), benzoic acid (TCI), cesium carbonate ($Cs_2CO_3$, TCI), and palladium on carbon (Pd/C, 10%, Sigma-Aldrich) were used as received. 1,2,4,5-Cyclohexanetetracarboxylic dianhydride (**CHDA**, Changzhou Sunlight Fine Chemicals Co., China) was dried in a vacuum oven at 120 °C for 12 h prior to use. 4,4′-Diaminodiphenyl ether (**ODA**, Changzhou Sunlight Fine Chemicals Co., China) and 4,4′-(hexafluoroisopropylidene) diphthalic anhydride (**6FDA**, Changzhou Sunlight Fine Chemicals Co., China) were purified by vacuum sublimation before use. *N,N*-Dimethylacetamide (DMAc, Tianjin Fuyu Fine Chemicals Co., China) and *N,N*-dimethylformamide (DMF, Tianjin Fuyu Fine Chemicals Co., China) were purified by vacuum distillation and dehydrated with 4 Å molecular sieves prior to use. Other solvents and reagents were used as received unless otherwise stated.

## Instruments

Fourier transform infrared (FT-IR) spectra were recorded on an FT-IR spectrophotometer (Bruker Tensor 27). $^1$H NMR and $^{13}$C NMR spectra were obtained on a Bruker Avance 400 MHz spectrometer (Bruker, Germany). The transmittance of the resulting films was measured using a TU-1901 UV–vis spectrophotometer in transmittance mode over the wavelength range of 200–800 nm. Mass spectra were recorded on a WATERS I-Class VION IMS QTof Mass Spectrometer (LC-TOF-MS) using Electron Spray Ionization (ESI) in positive ion mode. The number-average ($M_n$) and weight-average ($M_w$) molecular weight of the resulting PIs were determined by gel permeation chromatography (GPC, Waters 1515) with DMF as an eluent at room temperature at a flow rate of 1 mL min$^{-1}$. Polystyrene standards were used for calibration. Analyte samples were filtered through a nylon membrane with 0.22 μm pore size before injection. Thermal stability was carried out on a Mettler Toledo TGA2 synchronous thermal analyzer at a heating rate of 10 °C min$^{-1}$ under a nitrogen atmosphere from 30 °C to 800 °C. The glass transition temperatures ($T_g$s) of PI films were determined on a DMA 850 instrument at a programmed heating rate of 3 °C min$^{-1}$ at a frequency of 1 Hz from room temperature to 350 °C in a tensile mode. The coefficient of thermal expansion (CTE) of PI films in the glassy state was measured from 50 to 250 °C on a TMA 450 instrument at a heating rate of 5 °C min$^{-1}$ and a nitrogen flow rate of 50 mL min$^{-1}$ and the second heating cycle was used to calculate the CTE values. The mechanical properties (tensile strength, elongation at break, and tensile modulus) of the PI films were measured on an Instron tensile instrument according to ASTM D882-88 with 120 × 10 mm$^2$ specimens at a crosshead speed of 2 mm min$^{-1}$ at ambient temperature.

## Monomer synthesis

**4-(3-Methyl-4-nitrophenyloxy)aniline (*o*-M-NODA).** The synthetic route to ODA-based diamines is presented in Scheme 1. Take ***o*-M-NODA** as an example to illustrate the general synthetic procedures. Specifically, in a 250 mL three-necked round-bottom flask equipped with a stirring bar under a nitrogen atmosphere, 4-aminophenol (10.91 g, 0.1 mol), 5-fluoro-2-nitrotoluene (15.51 g, 0.1 mol) and $Cs_2CO_3$ (32.58 g, 0.1 mol)

 

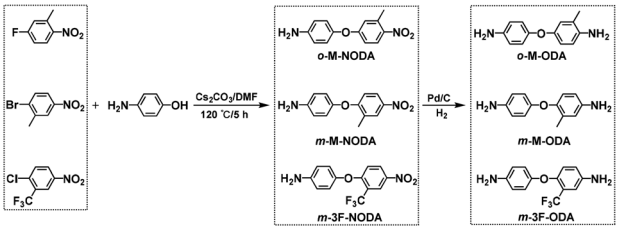


Scheme 1 Synthesis of three 4,4′-diaminodiphenyl ether (**ODA**)-based diamine monomers.

were dispersed in 120 mL of DMF. After stirring at 120 °C for 5 h in nitrogen, the mixture was cooled to room temperature and poured into 500 mL of distilled water. The precipitated solids were isolated *via* filtration, washed with copious water and dried in a vacuum oven at 80 °C for 12 h to give brown powdery crude products. The crude products were purified through flash silica gel column chromatography (dichloromethane/petroleum ether, v/v = 2 : 1) to yield the target compound (18.39 g, 82%). $^1$H NMR (400 MHz, $CDCl_3$, $\delta$, ppm) 7.85–8.20 (m, 1H), 6.84–6.91 (m, 2H), 6.75–6.81 (m, 2H), 6.69–6.75 (m, 2H), 3.69 (s, 2H), 2.58 (s, 3H). $^{13}$C NMR (100 MHz, DMSO-$d_6$, $\delta$, ppm) 162.77, 146.56, 143.75, 142.31, 136.55, 127.49, 121.43, 119.11, 114.95, 113.80, 20.67.

FT-IR (KBr): 3448 and 3371 cm$^{-1}$ ($-NH_2$), 2988 cm$^{-1}$ ($-CH_3$), 1581 and 1335 cm$^{-1}$ ($-NO_2$). ESI-MS ($m/z$): calcd for $[M + H]^+$: 245.09207, found: 245.09153.

**4-(2-Methyl-4-nitrophenyloxy)aniline (*m*-M-NODA).** ***m*-M-NODA** was prepared from 4-aminophenol and 2-bromo-5-nitrotoluene using the same procedure as that used for ***o*-M-NODA** (19.06 g, 85%). $^1$H NMR (400 MHz, DMSO-$d_6$, $\delta$, ppm) 8.17 (d, 1H), 8.01 (d, 1H), 6.75–6.88 (m, 2H), 6.66 (d, 3H), 5.13 (s, 2H), 2.37 (s, 3H). $^{13}$C NMR (100 MHz, DMSO-$d_6$, $\delta$, ppm) 162.83, 146.53, 144.02, 140.95, 127.68, 126.15, 123.40, 121.40, 114.97, 113.68, 15.86. FT-IR (KBr): 3416, 3317 and 3222 cm$^{-1}$ ($-NH_2$), 2922 cm$^{-1}$ ($-CH_3$), 1591 and 1339 cm$^{-1}$ ($-NO_2$). ESI-MS ($m/z$): calcd for $[M + H]^+$: 245.09207, found: 245.09180.

**4-(2-Trifluoromethyl-4-nitrophenyloxy)aniline (*m*-3F-NODA).** ***m*-3F-NODA** was prepared from 4-aminophenol and 2-chloro-5-nitrobenzotrifluoride using the same procedure as that used for ***o*-M-NODA** (25.65 g, 86%). $^1$H NMR (400 MHz, DMSO-$d_6$, $\delta$, ppm) 8.53–8.36 (m, 2H), 7.00 (d, 1H), 6.88 (d, 2H), 6.65 (d, 2H), 5.24 (s, 2H). $^{19}$F NMR (DMSO-$d_6$, $\delta$, ppm) −61.64. $^{13}$C NMR (100 MHz, DMSO-$d_6$ $\delta$, ppm) 161.81, 147.25, 143.13, 140.71, 129.89, 126.45, 123.74, 123.18, 123.13, 123.08, 123.02, 121.27, 121.03, 118.32, 118.00, 117.68, 117.36, 116.57, 114.99. FT-IR (KBr): 3494 and 3394 cm$^{-1}$ ($-NH_2$), 1598 and 1344 cm$^{-1}$ ($-NO_2$), 1127–1188 cm$^{-1}$ ($-CF_3$). ESI-MS ($m/z$): calcd for $[M + H]^+$: 299.0638, found: 299.06408.

**3-Methyl-4,4′-diaminodiphenyl ether (*o*-M-ODA).** ***o*-M-NODA** (5.61 g, 25 mmol) in THF (20 mL) was reduced using 10% Pd/C (0.28 g) in a pressure vessel under 10 bar of hydrogen for 6 h at room temperature. After removal of the catalyst and solvent, pure ***o*-M-ODA** was obtained in 91% yield (4.87 g) through flash silica gel column chromatography (dichloromethane/ethyl acetate, v/v = 10 : 1). $^1$H NMR (400 MHz, DMSO-$d_6$, $\delta$, ppm) 6.58–6.68 (m, 2H), 6.44–6.58 (m, 5H), 4.78 (s, 2H), 4.55 (s, 2H), 2.00 (s, 3H). $^{13}$C NMR (100 MHz, DMSO-$d_6$, $\delta$, ppm) 148.62, 148.51, 144.02, 141.93, 122.56, 120.01, 119.02, 116.39, 114.84, 114.77, 17.57. FT-IR (KBr): 3214–3451 cm$^{-1}$ ($-NH_2$), 2896 cm$^{-1}$ ($-CH_3$).

**2-Methyl-4,4′-diaminodiphenyl ether (*m*-M-ODA).** ***m*-M-ODA** was prepared from ***m*-M-NODA** using the same procedure as that used for ***o*-M-ODA** (4.82 g, yield: 90%). $^1$H NMR (400 MHz, DMSO-$d_6$, $\delta$, ppm) 6.45–6.56 (m, 5H), 6.43 (d, 1H), 6.35 (d, 1H), 4.73 (s, 4H), 2.00 (s, 3H). $^{13}$C NMR (100 MHz, DMSO-$d_6$, $\delta$, ppm) 149.49, 145.43, 144.56, 143.26, 129.30, 120.31, 117.18, 116.48, 114.99, 112.52, 16.13. FT-IR (KBr): 3210–3411 cm$^{-1}$ ($-NH_2$), 2910 cm$^{-1}$ ($-CH_3$).

**2-Trifluoromethyl-4,4′-diaminodiphenyl ether (*m*-3F-ODA).** ***m*-3F-ODA** was prepared from ***m*-3F-NODA** using the same procedure as that used for ***o*-M-ODA** (6.30 g, yield: 94%). $^1$H NMR (400 MHz, DMSO-$d_6$, $\delta$, ppm) 6.86 (d, 1H), 6.74 (d, 1H), 6.60–6.69 (m, 3H), 6.53 (d, 2H), 5.25 (s, 2H), 4.87 (s, 2H). $^{19}$F NMR (DMSO-$d_6$, $\delta$, ppm) −61.90.$^{13}$C NMR (100 MHz, DMSO-$d_6$, $\delta$, ppm) 147.92, 145.47, 144.67, 144.27, 127.87, 125.16, 122.46, 120.69, 120.32, 120.03, 119.74, 119.43, 119.12, 118.65, 114.83, 110.79, 110.74, 110.69, 110.64. FT-IR (KBr): 3199–3405 cm$^{-1}$ ($-NH_2$), 1045–1151 cm$^{-1}$ ($-CF_3$).

## Polymerization

Polyimides (PIs) were prepared *via* a conventional two-step chemical imidization as shown in Scheme 2. The compositions of the PIs are presented in Table 1. Poly(amic acid)s (PAAs) were prepared as the 20 wt% solid content of PAA in DMAc. The molar ratio of diamine, **CHDA** and **6FDA** was 2 : 1 : 1. The synthesis of **PI-1** was taken as an example to illustrate the general synthetic route as follows: **ODA** (10 mmol, 2.0024 g) and DMAc (10.49 g) were added into a 150 mL three-necked flask equipped with a mechanical stirrer under a nitrogen atmosphere. After **ODA** was completely dissolved, **CHDA** (5 mmol, 1.1208 g) and benzoic acid (5 mmol, 0.6106 g) in 8 g of DMAc was added dropwise by using a syringe pump in 1 h and then stirred at room temperature for 12 h. Afterwards, **6FDA** (5 mmol, 2.2212 g) and DMAc (2.88 g) were added to the reaction solution in one portion and further stirred for about 24 h at room temperature. After adding chemical imidization reagents (trimethylamine/acetic anhydride), the reaction solution was stirred for about 24 h at room temperature and then slowly poured into ethanol under vigorous stirring. The fibrous PI precipitates were filtered and washed twice with ethanol, and finally dried in a vacuum oven at 80 °C for 12 h. A homopolyimide, **PI-5**, was prepared as a reference sample by directly polymerizing ***m*-3F-ODA** with **6FDA** and without **CHDA** in DMAc as the 10 wt% solid content followed by chemical imidization (Scheme S1, ESI†).

## Film formation

PI powder was dissolved in DMF at a solid content of 15 wt%. The solution was filtered through a nylon filter with 0.22 μm pore size and then cast onto a levelled glass substrate. The

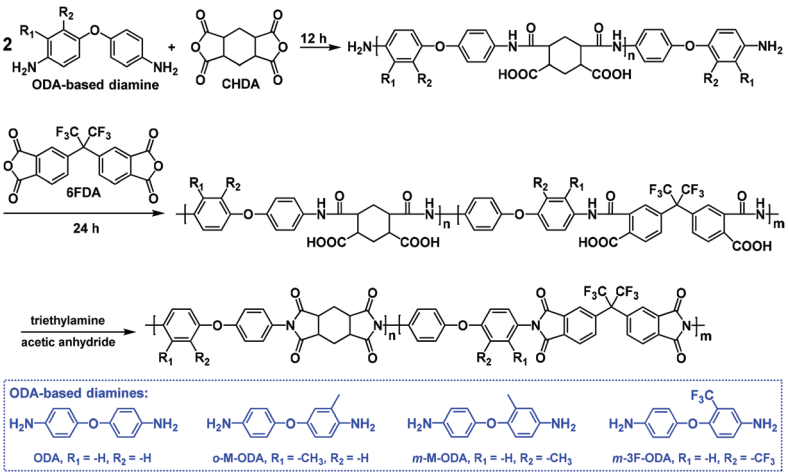


Scheme 2 Synthesis of copolyimides *via* a conventional two-step chemical imidization method.

Table 1 Compositions, inherent viscositiesand GPC data of the resulting polyimides

| Sample code[#] | Diamine | Dianhydride 1 | Dianhydride 2 | $\eta_{inh}$[a] (dL g$^{-1}$) | $M_n$ (g mol$^{-1}$) | $M_w$ (g mol$^{-1}$) | $M_w/M_n$ |
|---|---|---|---|---|---|---|---|
| **PI-1** | ODA | CHDA | 6FDA | 0.84 | 59 573 | 66 492 | 1.12 |
| **PI-2** | *o*-M-ODA | CHDA | 6FDA | 0.56 | 48 288 | 56 517 | 1.17 |
| **PI-3** | *m*-M-ODA | CHDA | 6FDA | 0.75 | 54 645 | 64 801 | 1.19 |
| **PI-4** | *m*-3F-ODA | CHDA | 6FDA | 0.73 | 69 715 | 76 281 | 1.09 |
| **PI-5** | *m*-3F-ODA | — | 6FDA | 1.72 | 73 739 | 82 256 | 1.12 |

[a] Inherent viscosities of PIs, determined in DMAc (0.5 g dL$^{-1}$) at 25 °C using an Ubbelohde viscometer.

solvent was slowly evaporated in a vacuum oven at 80 °C for 10 h and then heated to 160 °C for 4 h to remove the residual solvent and yield a free-standing film with a thickness of 40–50 μm.

## Results and discussion

### Monomer synthesis

Three **ODA**-based diamines with different substituents (–$CH_3$, –$CF_3$) and substitution positions (*ortho* position and *meta* position) in an aniline ring were prepared from aminophenol and halogenated nitrobenzene (as shown in Scheme 1). The structures of the target compounds were characterized through $^1$H NMR, $^{13}$C NMR and FT-IR spectroscopic techniques (Fig. S1–S16, ESI†). The results indicate the successful preparation of the target compounds.

### Polymerization

A conventional two-step procedure was adopted for the synthesis of PIs as shown in Scheme 2. To better isolate and identify the effect of **CHDA** on the comprehensive properties of the resulting PI films, a reference sample, that is, PI derived from ***m*-3F-ODA** and sole **6FDA** was also prepared (Scheme S1, ESI†). The compositions of the four obtained copolyimides and one homopolyimide are summarized in Table 1. **CHDA** in DMAc was added dropwise firstly to the solution of diamine to inhibit the chain growth, which is expected to result in amino-terminated macromolecules, rather than oligomers or homopolymer blocks. After **6FDA** was added and completely dissolved, the solution immediately became viscous, indicative of further polymer chain growth. Benzoic acid was herein used to increase the reactivity of **CHDA** upon reacting with diamine monomers. The imidization of PAA was carried out in the presence of triethylamine as a catalyst and acetic anhydride as a dehydrating agent. $^1$H NMR and FT-IR spectroscopy techniques were carried out to identify the backbone structures of the resulting PIs, and GPC measurement was utilized to monitor the relative molecular weight of the resulting PIs (Fig. S17, ESI†).

As shown in the $^1$H NMR spectra (Fig. S18, ESI†), the peaks at 7.7–8.3 ppm are related to the aromatic protons in **6FDA**, while the peaks at 6.5–7.6 ppm correspond to the aromatic protons in the diamine. The signals of alicyclic protons in **CHDA** locate at 3.24, 2.29 and 1.99 ppm, respectively. The absence of the characteristic resonances assigned to amic acid indicates the completion of imidization. Furthermore, the characteristic absorption bands of the five-membered imide ring at 1785 cm$^{-1}$ ($\nu_{as}$, C=O), 1720 cm$^{-1}$ ($\nu_s$, C=O), 1380 cm$^{-1}$ ($\nu$, C–N) and 721 cm$^{-1}$ ($\delta$, C=O) are observed in FT-IR spectra of the resulting PIs (Fig. S19, ESI†), while the typical peaks corresponding to the amic acid (1650 and 1535 cm$^{-1}$) are absent, which further confirmed the completion of imidization.[29] Additionally, the absorption bands at around

 

1860 $cm^{-1}$ and 3300–3500 $cm^{-1}$, respectively, which are assigned to the anhydride and free amine groups are not observed, suggesting the complete reaction of the monomers.

As shown in Fig. S7–S10 (ESI†), the amino groups close to the substituents respectively display the chemical shifts of 4.55 ppm (***o*-M-ODA**), 4.73 ppm (***m*-M-ODA**), 4.77 ppm (**ODA**) and 5.25 ppm (***m*-3F-ODA**), implying a decreasing trend in amino reactivity on the order of ***o*-M-ODA** > ***m*-M-ODA** > **ODA** > ***m*-3F-ODA**. However, judging from the intrinsic viscosity ($\eta_{inh}$) of the resulting PIs shown in Table 1, except for the reference sample **PI-5**, **PI-1** made using **ODA** as the diamine has the highest $\eta_{inh}$, while **PI-2** exhibits the lowest, contrary to the fact that ***o*-M-ODA** is the most reactive diamine in comparison to the other three. Additionally, PIs made using diamines possessing substituents ($-CH_3$, $-CF_3$) show lower $\eta_{inh}$ values than **PI-1**. For **PI-2**, its *ortho* methyl substituent displays the most pronounced steric hindrance which would impede the polymer chain growth during polymerization, finally leading to the lowest molecular weight determined by the GPC method (Table 1) and thus the lowest $\eta_{inh}$. It should be noted that $\eta_{inh}$ is also affected by the internal interactions (frictions) between a single polyimide chain and solvent molecules. For **PI-3** and **PI-4** with pendant methyl or trifluoromethyl groups, the steric hindrance originating from the substitutions would weaken the internal interactions between single polyimide chain and solvent molecules, consequently leading to decreased $\eta_{inh}$ values in comparison with that of **PI-1** (with no substituents), as shown in Table 1. **PI-5** made using sole **6FDA** anhydride shows the highest $\eta_{inh}$ value among all PIs. This is to say that alicyclic anhydride incorporation possibly has a role in decreasing the internal interactions between the polyimide main chain and solvent molecules.

As indicated, the resulting PIs possess moderate to high molecular weights with the weight-average molecular weights ($M_w$s) ranging from 56 517 g $mol^{-1}$ to 82 256 g $mol^{-1}$, confirming the successful chain growth after 6FDA addition. Size exclusion chromatography (SEC) in DMF also reveals a monomodal and narrow dispersity for all PIs (Fig. S17, ESI†). **PI-5** made using ***m*-3F-ODA** and **6FDA** exhibits the highest molecular weight, while **PI-1–PI-4** display decreased molecular weight, indicating that **CHDA** incorporation somewhat impedes the polymer chain growth due to its lower reactivity. Compared with **PI-1**, PIs with methyl substituents, that is, **PI-2** and **PI-3**, exhibit a decrease in their molecular weights. In particular, **PI-2** shows the lowest molecular weight, consistent with its lowest $\eta_{inh}$ value, possibly originating from the considerable steric hindrance of the *ortho* methyl substitution. It needs to be noted that ***m*-3F-ODA** based PIs, namely, **PI-4** and **PI-5**, demonstrate higher molecular weights than **PI-1**, **PI-2** and **PI-3**. This is contrary to the fact that ***m*-3F-ODA** has the lowest reactivity upon reacting with **6FDA**. As a matter of fact, SEC is an ideal technique to monitor the polymer molecular weight based on the size exclusion mechanism by comparing the size of the target polymer with a linear standard polymer (**PMMA** or **PS**). However, in our case, the steric trifluoromethyl incorporation into **PI-4** and **PI-5** would inevitably enlarge the molecular size of the polymer, consequently increasing the hydrodynamic volume and thus resulting in a reduction in retention time in the column of GPC, which would give an "enhanced" molecular weight of the polymer. This phenomenon can also be found in a few related investigations.[30–35]

The XRD patterns of the resulting PI films are shown in Fig. S20 (ESI†). The broad peaks of the resulting PI films indicate their amorphous nature.[36] Broad diffraction peaks centred at $2\theta$ = 15.61°, 15.52°, 15.37° and 15.14°, respectively, were observed for **PI-1**, **PI-2**, **PI-3** and **PI-4**, and the corresponding average interchain distances (*d*-spacings) were calculated to be 5.65 Å, 5.71 Å, 5.76 Å and 5.85 Å (Table 2).[29,37–40] The increase in the average interchain distance indicates that the substituent insertion would inhibit interchain stacking. By comparing **PI-2** with **PI-3**, it is found that **PI-3** demonstrates looser chain–chain packing density, albeit both their substituents are methyl groups. This is to say that the substituent in the *meta* position plays a more pronounced role in enlarging the interchain distance. Among the substituents in this study, the trifluoromethyl group is the bulkiest so that **PI-4** shows the largest *d*-spacing (5.85 Å). It is noteworthy that **PI-5** possessing a trifluoromethyl substituent displays the lowest *d*-spacing (5.55 Å) among the resulting PIs, suggesting that the alicyclic **CHDA** may also exert certain effects on the interchain distance, since its rigid and twisted molecular structure also has a role in the way the polymer chains are packed together.

### Optical transparency of the resulting PI films

The transmittance of the resulting PI films was measured using a UV–vis spectrophotometer with the wavelength ranging from 200 to 800 nm. As shown in Fig. 1 and Table 2, all PI films show excellent optical transparency with transmittance at 400 nm above 71% and cut-off wavelength ($\lambda_0$) ranging from 300 nm to 315 nm. The mechanism behind the excellent optical transparency should be mainly owing to the incorporation of alicyclic **CHDA**, which inhibits or weakens the formation of inter-/intramolecular CTCs and the electronic conjugation.[23,24,41,42] Notably, the substituent and its substitution position can also exert certain effects on the transmittance of the resulting PI films. By comparing **PI-2** with **PI-3**, both of which are derived from diamines with methyl groups but different substitution positions, however, **PI-2** exhibits much higher transmittance at 400 nm than that of **PI-3** (85.5% *vs.* 71.1%), although **PI-3** has a more pronounced interchain distance than **PI-2** (5.76 Å *vs.* 5.71 Å) and more suppressed CTCs can be expected within **PI-3**. This indicates that the steric *ortho* substitution possibly plays a more significant role in inhibiting the CTC formation (Scheme S2, ESI†).[2] It has been proved that fluorine introduction can effectively inhibit CTC formation and electron-conjugation due to its strong electron-withdrawing effect.[43,44] Therefore, the **PI-4** film derived from ***m*-3F-ODA** possesses superior optical transparency among all PIs with a transmittance at 400 nm of up to 86.8%. This result, coincidentally, is consistent with the largest interchain distance shown in Table 2. By contrast, **PI-5** shows slightly inferior transmittance at 400 nm (80.2%) in comparison with

Table 2 Optical transparency and *d*-spacing of the resulting PI films

| Sample code# | Cut-off wavelength[a] (nm) | Transmittance at 400 nm (%) | Transmittance at 800 nm (%) | *d*-Spacing[b] (Å) |
|---|---|---|---|---|
| **PI-1** | 314 | 71.4 | 90.3 | 5.65 |
| **PI-2** | 307 | 85.5 | 91.1 | 5.71 |
| **PI-3** | 313 | 71.1 | 90.7 | 5.76 |
| **PI-4** | 300 | 86.8 | 90.9 | 5.85 |
| **PI-5** | 315 | 80.2 | 89.7 | 5.55 |

[a] Cut-off wavelength indicates the wavelength with a transmittance of lower than 1%. [b] *d*-Spacing is calculated according to Bragg's law.

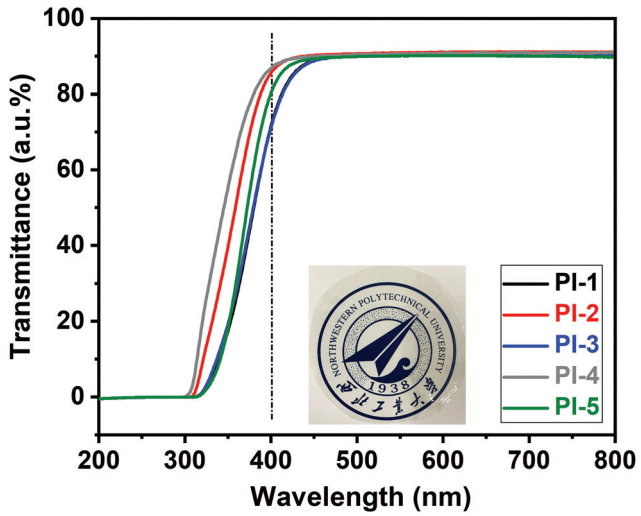


Fig. 1 Transmittance curves of the resulting PI films at UV–vis wavelength (the thickness of PI films was 20 ± 2 μm). The inset indicates the digital image of the **PI-4** film derived from **m-3F-ODA** diamine.

**PI-4**, albeit it is also prepared by using ***m*-3F-ODA**. This indicates that alicyclic **CHDA** cooperation with fluorine introduction can exert more positive effects on the optical properties of the PI films.

### Thermal properties of the resulting PI films

The thermal properties of the resulting PI films were measured by using DMA, TGA and TMA. As shown in Table 3 and Fig. 2, all PI samples exhibit good thermal properties, showing high $T_g$ values above 300 °C, $T_d$ values above 480 °C and CTE values ranging from 55 to 63 ppm $K^{-1}$. The thermal properties are

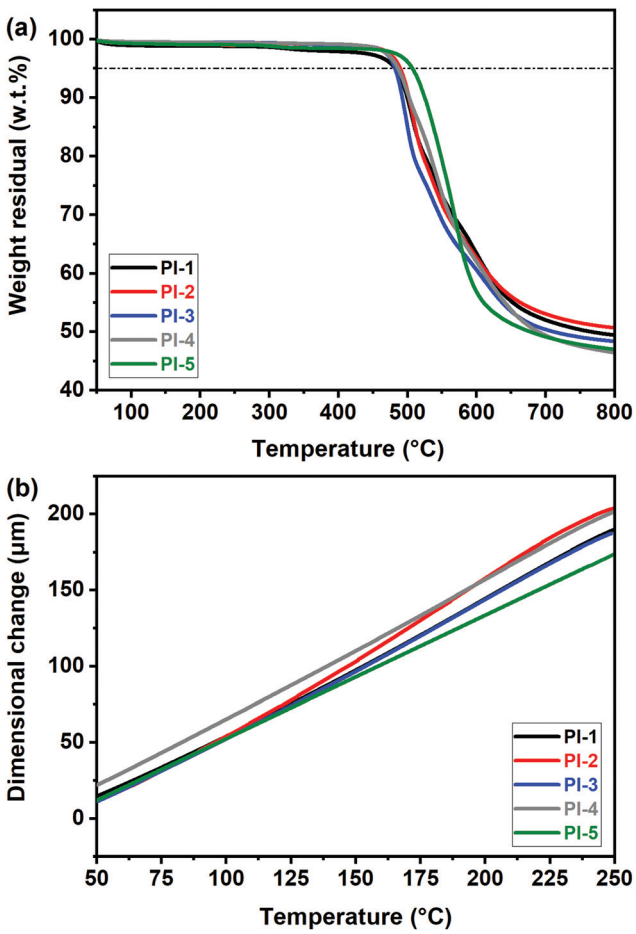


Fig. 2 TGA (a) and TMA (along the *X*–*Y* direction) and (b) curves of the resulting PI films.

Table 3 Mechanical and thermal properties of the resulting PI films

| Sample code# | Tensile modulus (GPa) | Tensile strength (MPa) | Elongation at break (%) | Toughness (MJ $m^{-3}$) | $T_g$[a] (°C) | $T_d$[b] (°C) | CTE[c] (ppm $K^{-1}$) |
|---|---|---|---|---|---|---|---|
| **PI-1** | 2.74 ± 0.10 | 102.0 ± 4.3 | 58.1 ± 12.1 | 50.0 ± 11.7 | 321 | 482 | 56.8 |
| **PI-2** | 3.58 ± 0.10 | 119.9 ± 4.6 | 6.3 ± 1.1 | 5.2 ± 1.4 | 324 | 489 | 62.8 |
| **PI-3** | 3.08 ± 0.09 | 106.8 ± 2.2 | 14.1 ± 2.2 | 9.6 ± 2.1 | 309 | 482 | 56.5 |
| **PI-4** | 2.76 ± 0.15 | 102.0 ± 1.0 | 16.3 ± 2.4 | 16.2 ± 2.8 | 308 | 486 | 57.8 |
| **PI-5** | 2.60 ± 0.06 | 102.1 ± 2.6 | 35.8 ± 4.6 | 32.3 ± 5.4 | 300 | 507 | 54.9 |

[a] The glass-transition temperature ($T_g$), determined in a tensile DMA mode at 5 °C $min^{-1}$ from room temperature to 350 °C. [b] Thermal decomposition temperature at 5% weight loss with a heating rate of 10 °C $min^{-1}$ under a nitrogen atmosphere. [c] Coefficient of thermal expansion along the *X*–*Y* direction, measured in the range of 50–250 °C at a heating rate of 5 °C $min^{-1}$.

 

comparable to those of some wholly aromatic PIs, whose $T_g$ values usually range from 250 °C to 400 °C, $T_d$ values from 450 °C to 500 °C, and CTE values from 40 to 60 ppm $K^{-1}$. These results indicate that the incorporation of a labile alicyclic moiety into PI backbones does not detrimentally decrease their thermal properties. It should be noted that **PI-2** shows the highest $T_g$ value. This is counterintuitive at the first glance since **PI-2** has the lowest $\eta_{inh}$ value and relative molecular weight as shown in Table 1. However, if we take a closer look at the sample, we can easily figure out that the effect of the steric hindrance of the methyl group on the segmental motions is not taken into account. The methyl in the *ortho* position can significantly prevent the single bond rotation and thus rigidify the polymer backbones. By contrast, substitutions in the *meta* position, as evidenced by the increased *d*-spacing shown in Table 2, can remarkably enlarge the interchain distance. As a result, the percentage of the free volume within **PI-3** and **PI-4** is increased, which favours the enhanced segmental motion, resulting in much lower $T_g$ values (309 °C for **PI-3** and 308 °C for **PI-4**). The thermal stability of a polymer is mainly related to the bond energy of covalent bonds that form the polymer. The resulting PIs, except the wholly aromatic **PI-5**, have similar structures, thus leading to comparable $T_d$s. As seen in Table 3, comparable CTEs are observed for **PI-1**, **PI-3**, **PI-4** and **PI-5**, while the largest for **PI-2**. In general, the CTE, indicative of dimensional stability, is mainly associated with the molecular chain rigidity (orientation degree) and chain–chain interaction. As discussed above, the lowest relative molecular weight in **PI-2** is prone to decreasing the chain–chain interaction (van der Waals' force). As a consequence, more pronounced thermal expansion may exist in **PI-2** at elevated temperatures. Notably, the CTE of a polymer tends to be inversely proportional to the degree of in-plane orientation of polymer chains. Therefore, making the PI chains highly oriented by utilizing biaxial stretching or other techniques during the film-formation process is believed to improve the dimensional stability. This investigation, however, is currently still on the way.

### Mechanical properties of the resulting PI films

Although alicyclic-based PIs hold great potential for developing flexible, colourless and ductile substrates for displays, the majority of the reported PIs thus far have undesirable mechanical properties (tensile strength less than 90 MPa, tensile modulus below 2.0 GPa and elongation at break no more than 10%),[16,25,26,45–48] which would impede their practical applications in flexible microelectronics. Therefore, it is of great significance to achieve high optical transparency while maintaining good mechanical strength and sufficient toughness. As shown in Fig. 3 and Table 3, all the resulting PI films fracture in a ductile manner and exhibit excellent mechanical properties with a tensile strength above 102 MPa and tensile modulus over 2.6 GPa. Interestingly, **PI-2** shows the highest tensile strength (*ca.* 120 MPa) and tensile modulus (3.58 GPa), although this sample has the lowest molecular weight (Table 1). **PI-2** demonstrates the lowest elongation at break

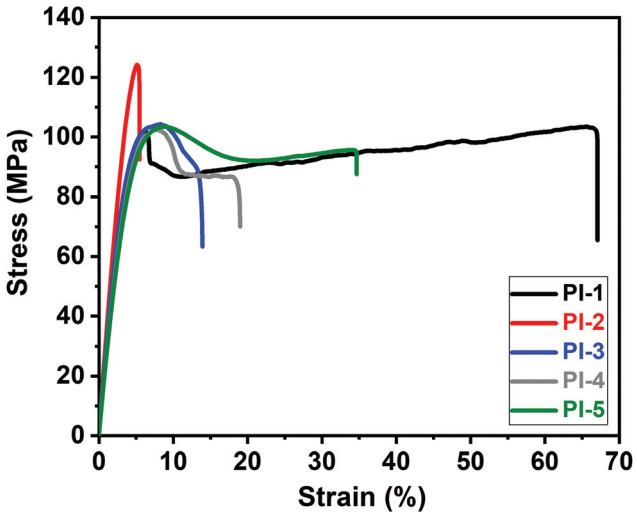


Fig. 3 Tensile stress–strain curves of the resulting PI films.

(6.3%) and toughness (5.2 MJ $m^{-3}$), consistent with its significant backbone rigidity and the restricted single bond rotation originating from the *ortho* methyl substitution. It is noteworthy that when ***m*-3F-ODA** is used, whose reactivity is the lowest, the prepared **PI-4** and **PI-5** counterintuitively exhibit admirable mechanical properties with a tensile strength up to 102 MPa, tensile modulus as high as 2.60–2.76 GPa, elongation at break more than 16%, and fracture toughness exceeding 16.2 MJ $m^{-3}$, since an increase of the fluorine content usually results in reduced chain–chain interaction and thus poor mechanical properties.[49,50] However, if we refer to the $\eta_{inh}$ values and relative molecular weights shown in Table 1, we can find that the $\eta_{inh}$ values of **PI-4** (0.73 dL $g^{-1}$) and **PI-5** (1.72 dL $g^{-1}$) are far higher than 0.5 dL $g^{-1}$, and the relative molecular weight ($M_n$) is about 70 kg $mol^{-1}$, suggesting a sufficiently high molecular weight, which might be responsible for the admirable mechanical strength.[25,38] Besides, **PI-1** shows superior flexibility with the elongation at break surprisingly reaching 58.1%, making **PI-1** exhibit superior fracture toughness as high as 50.0 MJ $m^{-3}$. To the best of our knowledge, this is the highest value of alicyclic-based PI films reported thus far. The impressive tensile properties with admirable heat resistance shown in Table 3 confirm the effectiveness and the applicability of our proposed "sequential addition" strategy.

### Solubility of the resulting PIs

The solubility of the resulting PIs was tested in organic solvents, and the results are summarized in Table 4. All these PIs show good solubility in polar aprotic organic solvents (DMSO, NMP, DMAc, DMF and THF) while demonstrating decreased solubility (insoluble or partially soluble) in $CHCl_3$ and $CH_2Cl_2$. Notably, PIs derived from diamines with substituents (**PI-2**, **PI-3**, **PI-4**) have preferable solubility compared with **PI-1**, mainly owing to the enlarged interchain distance (Table 2), allowing them to be solvated and easily dissolved. Owing to

Table 4 Solubility of the resulting PIs in this study[a]

| Sample code # | DMSO | NMP | DMAc | DMF | THF | $CHCl_3$ | $CH_2Cl_2$ |
|---|---|---|---|---|---|---|---|
| **PI-1** | ++ | ++ | ++ | ++ | ++ | −− | −− |
| **PI-2** | ++ | ++ | ++ | ++ | ++ | +− | +− |
| **PI-3** | ++ | ++ | ++ | ++ | ++ | +− | +− |
| **PI-4** | ++ | ++ | ++ | ++ | ++ | +− | +− |
| **PI-5** | ++ | ++ | ++ | ++ | ++ | ++ | ++ |

[a] DMAc: *N*,*N*-dimethylacetamide; DMF: *N*,*N*-dimethylformamide, DMSO: dimethyl sulfoxide; NMP: 1-methyl-2-pyrrolidinone; THF: tetrahydrofuran; $CHCl_3$: chloroform; $CH_2Cl_2$: dichloromethane; ++: soluble at room temperature; +−: partially soluble at room temperature; and −−: insoluble at room temperature. Qualitative solubility was determined using 50 mg of polymer in 1 mL of solvent at room temperature.



the high fluorine content, **PI-5** shows the best solubility. The excellent solubility, with decreased intrinsic viscosity (Table 1), makes the synthesized PIs promising for practical applications in flexible electronics by simple spin-coating or efficient, low-cost, and continuous roll-to-roll processes.

## Conclusions

In summary, three 4,4′-diaminodiphenyl ether (**ODA**)-based diamines with different substituents ($-CH_3$, $-CF_3$) and substitution positions (*ortho* and *meta* positions) in an aniline ring was successfully prepared. Four copolyimides were prepared by reacting **CHDA** and **6FDA** with different **ODA**-based diamines in a typical sequential reaction manner. The resulting PI films show high optical transparency, good thermal stability, superior mechanical strength and desirable solubility. It is found that incorporation of substituents is beneficial for enhancing the optical transparency and tensile strength as well as tensile modulus yet resulting in a slight reduction in elongation at break and fracture toughness. Additionally, the substituent in the *ortho* position could exert a stronger effect on the optical transparency and mechanical properties in comparison with the *meta* position substituent. Owing to the strong electron-withdrawing effect of the trifluoromethyl group, which can effectively inhibit the CTC formation and electron-conjugation, the **PI-4** film derived from ***m*-3F-ODA** exhibits the highest optical transparency among the resulting samples with a transmittance at 400 nm of up to 86.8%. This work provides a useful approach for the synthesis of functional PI films for advanced optical applications, which would have guide significance for the design of highly transparent, thermally stable and mechanically strong polymer substrates for flexible displays.

## Author contributions

Ruhe Lian: conceptualization, methodology, writing – original draft, formal analysis, data curation, and writing – review & editing. Xingfeng Lei: methodology, writing – review & editing, formal analysis validation, and funding acquisition. Yuyang Xiao: methodology and data analysis. Shuyu Xue: methodology and data analysis. Guo Xiong: methodology and data analysis. Zixiang Zhang: data analysis. Dong Yan: data analysis. Qiuyu Zhang: conceptualization, methodology, supervision, and funding acquisition.

## Conflicts of interest

There are no conflicts to declare.

## Acknowledgements

The authors are grateful for the financial support provided by the National Natural Science Foundation of China (Grant No. 51903208), the Project Funded by China Postdoctoral Science Foundation (Grant No. 2019M653733), the Joint Fund Project in Shaanxi Province of China (Grant No. 2019JLM-4, 2019JLM-22) and the Youth Innovation Team of Shaanxi Universities. We would like to thank the Analytical and Testing Center of Northwestern Polytechnical University for performing tests and characterization studies.

## References

1 Y.-W. Lim, J. Jin and B.-S. Bae, *Adv. Mater.*, 2020, **32**, 1907143.
2 K.-H. Nam, H. K. Choi, H. Yeo, N.-H. You, B.-C. Ku and J. Yu, *Polymers*, 2018, **10**, 630.
3 W. A. MacDonald, *J. Mater. Chem.*, 2004, **14**, 4.
4 R. Lian, X. Lei, Y. Chen and Q. Zhang, *J. Appl. Polym. Sci.*, 2019, **136**, 47771.
5 I. Gouzman, E. Grossman, R. Verker, N. Atar, A. Bolker and N. Eliaz, *Adv. Mater.*, 2019, **31**, 1807738.
6 M. A. B. Meador, S. Wright, A. Sandberg, B. N. Nguyen, F. W. Van Keuls, C. H. Mueller, R. Rodríguez-Solís and F. L. A. Miranda, *ACS Appl. Mater. Interfaces*, 2012, **4**, 6346.
7 D.-J. Liaw, K.-L. Wang, Y.-C. Huang, K.-R. Lee, J.-Y. Lai and C.-S. Ha, *Prog. Polym. Sci.*, 2012, **37**, 907.
8 X. F. Lei, Y. Chen, H. P. Zhang, X. J. Li, P. Yao and Q. Y. Zhang, *ACS Appl. Mater. Interfaces*, 2013, **5**, 10207.
9 X. Lei, Y. Chen, M. Qiao, L. Tian and Q. Zhang, *J. Mater. Chem. C*, 2016, **4**, 2134.
10 R. Lian, X. Lei, S. Xue, Y. Chen and Q. Zhang, *Appl. Surf. Sci.*, 2021, **535**, 147654.

 

11 V. B. Nam, J. Shin, A. Choi, H. Choi, S. H. Ko and D. Lee, *J. Mater. Chem. C*, 2021, **9**, 5652–5661.
12 Y. Zhuang, J. G. Seong and Y. M. Lee, *Prog. Polym. Sci.*, 2019, **92**, 35.
13 J.-H. Yen, Y.-J. Wang, C.-A. Hsieh, Y.-C. Chen and L.-Y. Chen, *J. Mater. Chem. C*, 2020, **8**, 4102.
14 Y. Watanabe, Y. Sakai, Y. Shibasaki, S. Ando, M. Ueda, Y. Oishi and K. Mori, *Macromolecules*, 2002, **35**, 2277.
15 Z. Lan, C. Li, Y. Yu and J. Wei, *Polymers*, 2019, **11**, 1319.
16 Y. Zhuang, R. Orita, E. Fujiwara, Y. Zhang and S. Ando, *Macromolecules*, 2019, **52**, 3813.
17 L. Yi, C. Li, W. Huang and D. Yan, *J. Polym. Sci., Part A: Polym. Chem.*, 2016, **54**, 976.
18 C. Yi, W. Li, S. Shi, K. He, P. Ma, M. Chen and C. Yang, *Sol. Energy*, 2020, **195**, 340.
19 N. Mushtaq, Q. Wang, G. Chen, B. Bashir, H. Lao, Y. Zhang, L. R. Sidra and X. Fang, *Polymer*, 2020, **190**, 122218.
20 H.-Y. Lu, C.-Y. Chou, J.-H. Wu, J.-J. Lin and G.-S. Liou, *J. Mater. Chem. C*, 2015, **3**, 3629.
21 H. Liu, L. Zhai, L. Bai, M. He, C. Wang, S. Mo and L. Fan, *Polymer*, 2019, **163**, 106.
22 L. Zhai, S. Yang and L. Fan, *Polymer*, 2012, **53**, 3529.
23 M. Hasegawa, D. Hirano, M. Fujii, M. Haga, E. Takezawa, S. Yamaguchi, A. Ishikawa and T. Kagayama, *J. Polym. Sci., Part A: Polym. Chem.*, 2013, **51**, 575.
24 X. Hu, J. Yan, Y. Wang, H. Mu, Z. Wang, H. Cheng, F. Zhao and Z. Wang, *Polym. Chem.*, 2017, **8**, 6165.
25 X. Hu, H. Mu, Y. Wang, Z. Wang and J. Yan, *Polymer*, 2018, **134**, 8.
26 J. Miao, X. Hu, X. Wang, X. Meng, Z. Wang and J. Yan, *Polym. Chem.*, 2020, **11**, 6009.
27 L. Wu, X. Wu, H.-R. Qi, Y.-C. An, Y.-J. Jia, Y. Zhang, X.-X. Zhi and J.-G. Liu, *Polym. Adv. Technol.*, 2021, **32**, 1061.
28 Y. Wang, J. Zhou, X. Chen, J. Sun and Q. Fang, *ACS Sustainable Chem. Eng.*, 2019, **7**, 11728.
29 X. Lei, M. Qiao, L. Tian, Y. Chen and Q. Zhang, *J. Phys. Chem. C*, 2016, **120**, 2548.
30 B. V. Schmidt, N. Fechler, J. Falkenhagen and J.-F. Lutz, *Nat. Chem.*, 2011, **3**, 234.
31 A. E. Cherian, F. C. Sun, S. S. Sheiko and G. W. Coates, *J. Am. Chem. Soc.*, 2007, **129**, 11350.
32 J. B. Beck, K. L. Killops, T. Kang, K. Sivanandan, A. Bayles, M. E. Mackay, K. L. Wooley and C. J. Hawker, *Macromolecules*, 2009, **42**, 5629.
33 O. Altintas, J. Willenbacher, K. N. Wuest, K. K. Oehlenschlaeger, P. Krolla-Sidenstein, H. Gliemann and C. Barner-Kowollik, *Macromolecules*, 2013, **46**, 8092.
34 B. S. Murray and D. A. Fulton, *Macromolecules*, 2011, **44**, 7242.
35 J. Zhang, J. Tanaka, P. Gurnani, P. Wilson, M. Hartlieb and S. Perrier, *Polym. Chem.*, 2017, **8**, 4079.
36 X. Xiao, X. Qiu, D. Kong, W. Zhang, Y. Liu and J. Leng, *Soft Matter*, 2016, **12**, 2894.
37 Y. Chen, Q. Zhang, W. Sun, X. Lei and P. Yao, *J. Membr. Sci.*, 2014, **450**, 138.
38 Z. Wang, D. Wang, F. Zhang and J. Jin, *ACS Macro Lett.*, 2014, **3**, 597.
39 H. Gao, D. Yorifuji, Z. Jiang and S. Ando, *Polymer*, 2014, **55**, 2848.
40 J. Fang, H. Kita and K.-I. Okamoto, *J. Membr. Sci.*, 2001, **182**, 245.
41 K. Kanosue, T. Shimosaka, J. Wakita and S. Ando, *Macromolecules*, 2015, **48**, 1777.
42 C.-P. Yang and Y.-Y. Su, *Polymer*, 2005, **46**, 5797.
43 M. Hasegawa, K. Kasamatsu and K. Koseki, *Eur. Polym. J.*, 2012, **48**, 483.
44 M. Hasegawa, *Polymers*, 2017, **9**, 520.
45 T. Matsumoto and T. Kurosaki, *React. Funct. Polym.*, 1996, **30**, 55.
46 T. Matsumoto, S. Kawabata and R. Takahashi, *High Perform. Polym.*, 2006, **18**, 719.
47 S. V. Kumar, H.-C. Yu, J. Choi, K. Kudo, Y.-H. Jang and C.-M. Chung, *J. Polym. Res.*, 2011, **18**, 1111.
48 M. Hasegawa, M. Horiuchi and Y. Wada, *High Perform. Polym.*, 2007, **19**, 175.
49 D. Yin, Y. Li, H. Yang, S. Yang, L. Fan and J. Liu, *Polymer*, 2005, **46**, 3119.
50 F. Yang, J. Zhao, Y. Li, S. Zhang, Y. Shao, H. Shao, T. Ma and C. Gong, *Eur. Polym. J.*, 2009, **45**, 2053.